

# Electrostatic force microscopy of silver nanocrystals with nanometer-scale resolution

Ralph M. Nyffenegger and Reginald M. Penner<sup>a)</sup>

Department of Chemistry, Institute for Surface and Interface Science, University of California Irvine, Irvine, California 92697-2025

Rainer Schierle

Park Scientific Instruments, Sunnyvale, California 94089-1304

(Received 27 June 1997; accepted for publication 6 August 1997)

Silver nanoparticles on graphite basal plane surfaces were concurrently imaged using electrostatic force microscopy (EFM) and noncontact atomic force microscopy. EFM images were obtained having a lateral resolution of 4–5 nm, and a resolution perpendicular to the surface of  $\approx 1$  nm. The dependence of the contrast in the EFM data for the silver nanoparticles as a function of the applied tip bias was consistent with a positive charge for the silver nanocrystals on the graphite surface, qualitatively as expected by theory. © 1997 American Institute of Physics.

[S0003-6951(97)04039-4]

The electrostatic force microscope (EFM) maps the spatial variation of the potential-energy difference between a tip and a sample, which results from nonuniform charge distribution and variations in surface work function.<sup>1,2</sup> The range of applicability of the EFM is extended by its ability to image surface charge distributions resulting from subsurface structures such as  $p$ - $n$  junctions. Relative to most other scanning probe microscopy (SPM) methods, the contrast mechanism in EFM is well understood (see, for example, Belaidi *et al.*,<sup>3</sup> Hochwitz *et al.*,<sup>4</sup> Sarid,<sup>5</sup> and references cited therein) and the interpretation of EFM image data is, therefore, relatively straightforward. Unfortunately, the smallest resolvable features seen in the EFM images so far have been in the 50–100 nm range,<sup>6</sup> whereas other SPM modes such as noncontact (NC) atomic force microscopy (AFM) have routinely achieved much better lateral resolutions of  $\approx 5$  nm or less.<sup>7</sup> From a theoretical standpoint, nanometer-scale resolution should be obtainable using EFM provided that tip-sample distances below 10 nm are employed in order to minimize the contribution from the shaft of the tip or the cantilever itself.<sup>3</sup>

In this letter, we demonstrate that the  $\approx 5$  nm scale lateral resolution expected theoretically can be experimentally obtained. We have employed a sample surface on which the surface charge should be modulated on the nanometer scale consisting of silver nanoparticles having a mean diameter of 20–30 Å and disposed at a coverage of  $\approx 10^9$  cm<sup>-2</sup> on the atomically smooth graphite basal plane surface.<sup>8</sup> Because the disparate work functions of silver and graphite ( $\phi_{\text{Ag}} \approx 4.5$  eV, versus  $\phi_{\text{HOPG}} = 5.0$  eV), individual silver nanoparticles on this surface are expected to be positively charged.

Silver nanoparticles were deposited on graphite basal plane surfaces using a previously described electrochemical method.<sup>8</sup> All EFM experiments were performed in air using commercially available instruments (M5 or CP from Park Scientific Instruments, Sunnyvale, CA). The experimental parameters for EFM measurements were as follows: The force gradient was measured using a lock-in amplifier and an

ac bias of  $\approx 17$  kHz and 5 V rms amplitude. This frequency is well isolated from mechanical resonances of the microscope head and from the subharmonics of the cantilever driving frequency employed for concurrent noncontact AFM measurements of the surface topography. In addition, it is high enough to provide a sufficient bandwidth for the feedback circuit. The bias modulation was either applied at the heavily doped silicon tip<sup>9</sup> or at the sample, in either case, the other electrode (either sample or tip) was grounded. To this 17 kHz bias modulation a dc bias was added, ranging between  $\pm 10$  V. The topography was measured by monitoring a constant amplitude of oscillation of the cantilever at its resonance frequency, i.e., in the range of 90–400 kHz. Other imaging parameters were chosen to yield an amplitude of oscillation for the tip of 3–4 nm and a tip-sample distance of  $\approx 5$  nm. The scan rate was 0.3 Hz for window sizes up to  $1 \times 1 \mu\text{m}^2$ .

According to Terris *et al.*,<sup>10</sup> the electrostatic force,  $F$ , is given by a capacitive and a Coulombic term. The Coulombic term consists of a charge component induced by the applied voltage  $Q_e = CV$  and of a component due to a surface charge  $Q_s$ . The charge in the tip can then be written as  $Q_t = -(Q_s + Q_e)$ . The electrostatic force is given by

$$F \approx \frac{\delta C}{\delta d} \cdot \frac{v^2}{2} + \frac{Q_s Q_t}{4 \pi \epsilon_0 \epsilon_r d^2}, \quad (1)$$

$$F \approx \frac{\delta C}{\delta d} \cdot \frac{v^2}{2} - \frac{Q_s^2}{4 \pi \epsilon_0 \epsilon_r d^2} - \frac{Q_s CV}{4 \pi \epsilon_0 \epsilon_r d^2}. \quad (2)$$

The externally applied potential difference between the tip and sample,  $V$ , has both ac and dc components:  $V = V_{\text{dc}} + V_{\text{ac}} \cdot \sin(\omega t)$ . Substituting for  $V$  in Eq. (2) we obtain

$$F \approx \frac{\delta C}{\delta d} \cdot \frac{v_{\text{dc}}^2}{2} + \frac{\delta C}{\delta d} \cdot \frac{v_{\text{ac}}^2}{4} - \frac{Q_s^2}{4 \pi \epsilon_0 \epsilon_r d^2} - \frac{Q_s CV_{\text{dc}}}{4 \pi \epsilon_0 \epsilon_r d^2} + \left( \frac{\delta C}{\delta d} V_{\text{dc}} - \frac{Q_s C}{4 \pi \epsilon_0 \epsilon_r d^2} \right) \cdot V_{\text{ac}} \sin(\omega t) + \frac{\delta C}{\delta d} \cdot \frac{v_{\text{ac}}^2}{4} \cdot \cos(2\omega t). \quad (3)$$

<sup>a)</sup>Electronic mail: rmpenner@uci.edu

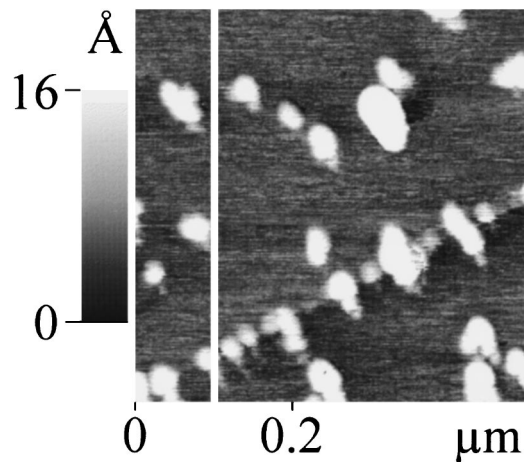


FIG. 1. NC-AFM image showing the topography of electrochemically deposited silver nanoparticles having an average height of  $\approx 20$  Å on graphite. The image window is  $0.5 \times 0.5 \mu\text{m}^2$  and was recorded at 0.3 Hz. As commonly observed, an increased density of particles can be found along the step edge, whereas on the basal plane a smaller areal density of particles is seen. The white line indicates where the cross sections in Fig. 3 were acquired.

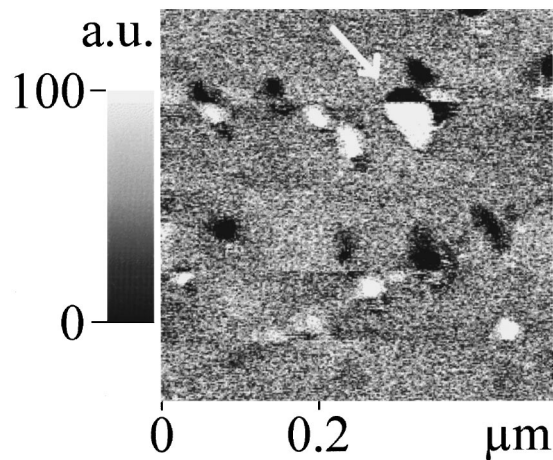


FIG. 2. Electrostatic force microscope signal acquired concurrently with the topography image of Fig. 1. The image has been processed by means of a line-by-line subtraction in order to remove large steps, which were introduced by the dc bias steps that were applied during the image acquisition. As indicated by the arrow, the contrast of a silver particle inverts relative to background as the sign of the applied dc bias changes. In this instance, the bias was switched from +10 to  $-8$  V.

Because the lock-in amplifier is referenced to the frequency  $\omega$ , the measured force will be sensitive to both the sign and the magnitude of the applied dc bias,  $V_{\text{dc}}$ , as well as to the surface charge on the sample,  $Q_s$ . As already indicated, the lower work function of silver versus graphite should result in  $Q_s > 0$ , and a contrast between graphite and silver can, thus, be expected in the EFM images of this surface.

In Fig. 1 is shown a typical NC-AFM image of silver nanoparticles on graphite. Previous work<sup>8</sup> has shown these particles to be approximately hemispherical, and the apparent height of these particles, obtained from the NC-AFM image data (20 Å, in this case), provides an excellent estimate of the particle radius. As a consequence of the finite size of the silicon tip, however, the apparent particle diameter obtained from the NC-AFM image data is much greater than the radius, approximately 400 Å in the NC-AFM image of Fig. 1, for example. An EFM image was concurrently acquired with the topographic image of Fig. 1, and this image is shown in Fig. 2 after a line-by-line background subtraction procedure. As the EFM image of Fig. 2 was acquired, the applied bias  $V_{\text{dc}}$  was stepped to five different values in the range from +10 to  $-10$  V as indicated in the plot of Fig. 3, which shows  $V_{\text{dc}}$  together with the corresponding EFM signal plotted along the slow scan direction.

Several conclusions can be derived from this experiment: First, the contrast and signal to noise of the topographical NC-AFM data of Fig. 1 are completely unaffected by the value of the applied bias  $V_{\text{dc}}$ . Second, the contrast of the silver particles with respect to the graphite substrate changes dramatically as a function of the applied bias  $V_{\text{dc}}$ , and an inversion of the EFM contrast is seen to coincide with a change in sign of  $V_{\text{DC}}$ . The contrast seen in this EFM image is, in fact, consistent with positively charged silver particles: For example, at the positive tip biases (versus sample), which were applied at the top of the image of Fig. 2, silver particles appear as protrusions from the surface because the positive charge on the tip, and the positively

charged particles interact repulsively. Finally, in terms of the image resolution, the images of Figs. 1 and 2 are comparable. If the lateral resolution is taken to equal the full width at half-maximum height of the smallest protrusion seen in the NC-AFM image, which is also resolved in the EFM image of Fig. 2, then a value of 4–5 nm is the approximate value that is achieved. A vertical resolution, defined as  $2\sigma$  (where  $\sigma$  is the rms noise in the EFM signal measured at clean regions of the graphite substrate), was approximately 1 nm. These values are comparable to the resolutions that are attainable using a variety of other SPM imaging modes, including lateral force microscopy and noncontact atomic force microscopy. Thus, it is demonstrated that with optimization of the EFM image acquisition parameters, essentially tip size-limited lateral resolution of a few nanometers is obtainable using electrostatic force microscopy.

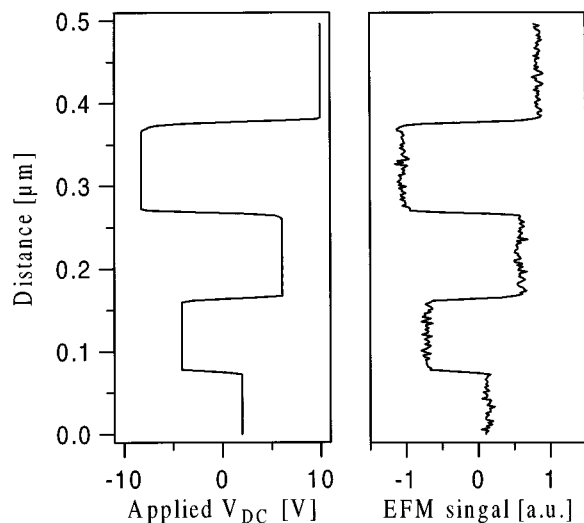


FIG. 3. The applied dc bias (left) and the unprocessed EFM signal (right) plotted as a function of position in the slow scan direction. The expected correlation between the sign and the amplitude of the applied dc bias and the resulting EFM signal is seen.

We have sometimes witnessed large differences between the topographic image of a graphite surface and the EFM image. Although the origin of these differences are incompletely understood at present, these data emphasize the excellent isolation that exists for topographical and electrostatic signals acquired from the same surface.

In summary, silver nanoparticles dispersed on graphite have been imaged using electrostatic force microscopy at a lateral resolution of 4–5 nm, and with a vertical resolution of about a nanometer. The contrast seen experimentally for these particles as a function of the applied imaging bias,  $V_{dc}$  is qualitatively consistent with theory for particles carrying a positive surface charge. In the case of the silver–graphite system, the accumulation of a positive charge on the silver particles is a consequence of the lower work function of silver as compared with the graphite basal plane. This work function disparity should be exaggerated for silver nanoparticles, which are expected to possess a work function below that of bulk silver ( $\phi_{Ag} \approx 4.5$  eV). A further, more complete, description of the mechanism of charge localization on nanoscopic metal and semiconductor particles awaits the acquisition of EFM data for mixed surfaces on which particles of two different materials having known, and different, work functions are present.

At UCI, this work was supported by the Office of Naval

Research, under Grant No. N00014-93-1-0757, and the NSF Young Investigator's Program, under Grant No. DMR-9257000. In addition, the following are gratefully acknowledged: The Funding of the Swiss National Science Foundation (R.M.N.), an A. P. Sloan Fellow, an Arnold and Mabel Beckman Young Investigator award, and a Camille Dreyfus Teacher–Scholar award (R.M.P.).

<sup>1</sup>Y. Martin, D. W. Abraham, and H. K. Wickramasinghe, *Appl. Phys. Lett.* **52**, 1103 (1988).

<sup>2</sup>J. E. Stern, B. D. Terris, H. J. Mamin, and D. Rugar, *Appl. Phys. Lett.* **53**, 2717 (1988).

<sup>3</sup>S. Belaidi, P. Girard, and G. Leveque, *J. Appl. Phys.* **81**, 1023 (1997).

<sup>4</sup>T. Hochwitz, A. K. Henning, C. Levey, C. Daghljan, and J. Slinkman, *J. Vac. Sci. Technol. B* **14**, 457 (1996).

<sup>5</sup>Dror Sarid, *Scanning Force Microscopy: With Applications to Electric, Magnetic, and Atomic Forces* (Oxford University Press, New York, 1994).

<sup>6</sup>T. Hidaka, T. Maruyama, M. Saitoh, N. Mikoshiba, M. Shimizu, T. Shiosaki, L. A. Wills, R. Hiskes, S. A. Dicarolis, and J. Amano, *Appl. Phys. Lett.* **68**, 2358 (1996).

<sup>7</sup>Yu N. Moiseev, V. M. Mostepanenko, V. I. Panov, and I. Yu Sokolov, *Phys. Lett. A* **132**, 354 (1988).

<sup>8</sup>J. V. Zoval, R. M. Stiger, P. R. Biernacki, and R. M. Penner, *J. Phys. Chem.* **100**, 837 (1996).

<sup>9</sup>Silicon tips are degeneratively doped semiconductors.

<sup>10</sup>B. D. Terris, J. E. Stern, D. Rugar, and H. J. Mamin, *Phys. Rev. Lett.* **63**, 2669 (1989).